


## Article

# The Removal of Crystal Violet from Textile Wastewater Using Palm Kernel Shell-Derived Biochar

Phyo Phyo Kyi <sup>1,†</sup>, Jude Ofei Quansah <sup>1,†</sup>, Chang-Gu Lee <sup>2</sup>, Joon-Kwan Moon <sup>3,\*</sup> and Seong-Jik Park <sup>4,\*</sup> 

<sup>1</sup> Department of Chemical Engineering, Hankyong National University, Anseong 17579, Korea; phyophyokyi17@gmail.com (P.P.K.); judequansah2018@gmail.com (J.O.Q.)

<sup>2</sup> Department of Environmental and Safety Engineering, Ajou University, Suwon 16499, Korea; changgu@ajou.ac.kr

<sup>3</sup> Department of Plant and Environmental Science, Hankyong National University, Anseong 17579, Korea

<sup>4</sup> Department of Bioresources and Rural System Engineering, Hankyong National University, Anseong 17579, Korea

\* Correspondence: jkmoon@hknu.ac.kr (J.-K.M.); parkseongjik@hknu.ac.kr (S.-J.P.); Tel.: +82-31-670-5083 (J.-K.M.); +82-31-670-5131 (S.-J.P.)

† These authors contributed equally to this work.

Received: 7 March 2020; Accepted: 24 March 2020; Published: 26 March 2020



**Abstract:** In this study, we explored the adsorption potential of biochar derived from palm kernel shell (BC-PKS) as an affordable adsorbent for the removal of crystal violet from wastewater. Kinetics, equilibrium, and thermodynamics studies were carried out to evaluate the adsorption of crystal violet onto BC-PKS. The kinetics adsorption process followed the pseudo-second-order model, indicating that the rate of adsorption is principally controlled by chemisorption. The adsorption equilibrium data were better fitted by the Langmuir isotherm model with a determination coefficient of 0.954 and a maximum adsorption of 24.45 mg/g. Thermodynamics studies found the adsorption of crystal violet by BC-PKS to be endothermic with increasing randomness at the BC-PKS/crystal violet interface. The percentage removal and adsorption capacity increased with the pH of the solution, as the negative charges on the biochar surface at high pH enhance the electrostatic attraction between crystal violet molecules and BC-PKS. Increasing the BC-PKS dosage from 0.1 to 1.0 g increased percent removal and decreased the adsorption capacity of crystal violet onto BC-PKS. Therefore, biochar from agricultural by-products, i.e., palm kernel shell, can be cost-effective adsorbents for the removal of crystal violet from textile wastewater.

**Keywords:** biochar; adsorption; crystal violet; palm kernel shell; agricultural byproduct

## 1. Introduction

Wastewater from paper, textile, cosmetics, food processing, and plastic producing industries contain various kinds of organic and harmful substances such as dyes [1]. Dyes such as crystal violet (CV) are composed of many functional groups that are stable and difficult to decompose because of their aromatic nature [2,3]. CV is used for making black and blue inks in ball-point pens and in printer ink jet manufacturing industrials [4]. Color paints, pharmaceuticals, leather, detergents, fertilizers, varnish, and waxes are also manufactured from CV [5–7]. However, CV, similar to most dyes, is a toxic carcinogenic with a recalcitrant classification because of its non-biodegradability, persistence in various environments, and poor microbial metabolism [7–9]. Furthermore, CV causes undesirable colorations of water bodies, resulting in low light penetration for photosynthetic activities, which affects aquatic life such as the growth of tumors in fish [10,11]. Consequently, the removal of

CV from wastewater before discharge must be implemented for the survival of both humans and aquatic organisms.

Recently, many technologies such as ion exchange [12], ozonation [12], coagulation [13], membrane filtration [14–16], catalytic degradation [17,18], precipitation [19], electrochemical treatment [20], and adsorption [21–25] have been investigated for the removal of dyes in wastewater. However, most of these treatments methods are expensive and require large amounts of energy [26]. Therefore, adsorption has been considered attractive due to its ease of operation and high effectiveness [27]. Adsorption should involve the use of low-cost, environmental friendly, and high-capacity adsorbents [28].

Biochar is a product of the biomass pyrolytic process with high-compact structure and dense surface functional groups that are responsible for its high adsorption capacity and surface reactivity [29,30]. Unlike highly efficient commercial activated carbon used in wastewater treatment, biochar has low economic viability. Therefore, new raw materials must be explored [31]. Many researchers have focused on the use of agricultural byproducts for the production of biochar because they are readily available, recyclable, less expensive, and easy to handle [32–37]. Biochar has been prepared from materials such as cabbage waste [38], mango leaves [39], woody trees [40], sugarcane [41], mushrooms [42], rice bran [43], corncoobs [44], peanut shells [45], date seeds [46], pine sawdust [47], coir pith [48], and dew melon peel [49] and has demonstrated a high adsorption capacity for the removal of contaminants.

Palm oil mills processing involve the production of mesocarp fiber and kernel shells [50]. The palm kernel shell (PKS) discarded as waste is chemically stable, insoluble, rich in functional groups [51], and a good candidate for the production of biochar [52,53]. Additionally, we know of no works on the use of biochar prepared from PKS (BC-PKS) for the removal of CV dye.

Therefore, this study explored to examine the applicability of BC-PKS for the removal of CV from textile wastewater. Additionally, kinetics, equilibrium, and thermodynamic studies were conducted under batch experiment conditions. Finally, the effect of solution pH and competitive cations on adsorption efficiency was also examined.

## 2. Materials and Methods

### 2.1. Solution Preparations

CV dye ( $\geq 90.0\%$  anhydrous basis, Sigma-Aldrich, Missouri, USA), HCl ( $\geq 99\%$  purity, Samchun Chemicals Co., Korea), NaOH ( $\geq 98\%$  purity, Samchun Chemicals Co., Korea), NaCl ( $\geq 99.5\%$  purity, Samchun Chemicals Co., Korea),  $\text{CaCl}_2$  (powder  $97\%$  purity, Daejung Chemicals and Metals Co., Korea),  $\text{AlCl}_3$  ( $99\%$  purity, Junsei Chemical Co., Japan),  $\text{NaNO}_3$  ( $\geq 99\%$  purity, Daejung Chemicals and Metals Co., Korea),  $\text{Na}_2\text{SO}_4$  ( $\geq 99\%$  anhydrous, Daejung Chemicals and Metals Co., Korea), and  $\text{NaHCO}_3$  ( $\geq 99.7\%$  purity, Samchun Chemicals Co., Korea) were used in this study. A stock solution of  $1000 \text{ mg/L}$  CV was prepared by the dissolution  $1 \text{ g}$  of dye with  $1 \text{ L}$  of distilled water in a volumetric flask. The stock solution was stored in a dark place to prevent depolarization. All solutions with the desired concentrations used in this study were prepared according to APHA [54].

### 2.2. Preparation of Biochar from Palm Kernel Shell

The BC-PKS used in this study was obtained from Design Factory Company (South Korea). As described in a previous study [55], BC-PKS was produced at a temperature of  $350^\circ\text{C}$  in a rotary kiln for  $20 \text{ min}$  after the extraction of the palm oil. The BC-PKS was crushed and screened using  $0.85$  to  $1.18 \text{ mm}$  sieves. After washing with deionized water to remove impurities, the BC-PKS was dried at  $105^\circ\text{C}$  for  $24 \text{ h}$  and stored in a desiccator until use.

### 2.3. Batch Adsorption Experiments

The removal of CV by BC-PKS was investigated under batch conditions. Batch experiments were conducted by reacting  $0.5 \text{ g}$  of BC-PKS with  $30 \text{ mL}$  of dye solutions in a  $50 \text{ mL}$  conical tube with an agitation speed of  $100 \text{ rpm}$  and temperature of  $25^\circ\text{C}$  in a shaking incubator, unless otherwise stated.

Kinetic analyses were carried out by varying the reaction time from 0.5 h to 24 h using the initial CV concentration (400 mg/L). Equilibrium batch experiments were performed using different initial CV concentrations (50–500 mg/L); the samples were analyzed after a 24 h reaction. Thermodynamic adsorption investigations were carried out by reacting 0.5 g of BC-PKS with 30 mL of 400 mg/L CV solution at reaction temperatures of 15, 25, and 35 °C for 24 h. The effect of the pH of the solution on the adsorption of CV was investigated at different pH levels. The pH of each solution was adjusted from 2 to 10 using 0.1 M HCl and 0.1 M NaOH and measured using a pH meter (9107BN, Thermo Scientific, MA, USA). The impact of BC-PKS doses on CV adsorption was explored by reacting different dosages of BC-PKS (0.1, 0.3, 0.5, 0.7, 0.9, and 1.0) g with 30 mL of 400 mg/L CV solution. The effects of competitive cations on the adsorption of CV by BC-PKS was investigated using 1 mM and 10 mM of NaCl, CaCl<sub>2</sub>, and AlCl<sub>3</sub> in a solution of 400 mg/L CV concentration reacting with 0.5 g of BC-PKS.

After the reaction, the samples were centrifuged to separate the CV solution from BC-PKS using a centrifuge (Combi 514R, Hanil Science Industrial Co., Ltd., Korea). The residual concentrations of CV dye were analyzed using a UV-visible spectrophotometer (Optizen POP QX, Mecasys, Korea) at a wavelength of 590 nm. All the experiments were carried out in triplicates.

#### 2.4. Data Analysis

The kinetic data were analyzed using the pseudo-first- and second-order-models [55,56]

$$q_t = q_e(1 - e^{-k_1 t}), \quad (1)$$

$$q_t = \frac{k_2 q_e^2 t}{1 + k_2 q_e t}, \quad (2)$$

where  $q_t$  is the amount of adsorbed CV (mg/g) per unit mass of BC-PKS at time  $t$ ,  $q_e$  is the amount of adsorbed CV (mg/g) per unit mass of BC-PKS when equilibrium is reached,  $k_1$  is a pseudo-first-order rate constant (1/h), and  $k_2$  is a pseudo-second-order rate constant (g/mg/h). The results of isothermal adsorption experiments were analyzed using the Langmuir (Equation (3)) and Freundlich (Equation (4)) models [55–57]

$$q_e = \frac{Q_m K_L C_e}{1 + K_L C_e}, \quad (3)$$

$$q_e = K_F C_e^{\frac{1}{n}}, \quad (4)$$

where  $C_e$  is the concentration of CV in the aqueous solution at equilibrium (mg/L),  $K_L$  is the Langmuir adsorption constant (L/mg) related to the binding energy,  $Q_m$  is the maximum adsorption amount (adsorption capacity in mg/g),  $K_F$  is the distribution coefficient (L/g), and  $n$  is the Freundlich constant. All parameters of the models were estimated using Sigma-Plot 10.0.

The thermodynamic characteristics of the adsorption experiments were analyzed using the following equations [23,55,56]:

$$\Delta G^0 = \Delta H^0 - T\Delta S^0, \quad (5)$$

$$\Delta G^0 = -RT \ln K_e, \quad (6)$$

$$\ln K_e = \frac{\Delta S^0}{R} - \frac{\Delta H^0}{RT}, \quad (7)$$

$$K_e = \frac{\alpha q_e}{C_e}, \quad (8)$$

where  $\Delta G^0$  is the change in Gibb's free energy (kJ/mol),  $\Delta S^0$  is the change in entropy (J/mol K),  $\Delta H^0$  is the change in enthalpy (kJ/mol),  $R$  is the ideal gas constant (J/mol K),  $K_e$  is the equilibrium constant, and  $\alpha$  is the amount of BC-PKS (g/L).  $\Delta S^0$  and  $\Delta H^0$  are obtained from the relationship between  $\ln K_e$  and  $1/T$  in Equation (7).

### 3. Results and Discussion

#### 3.1. Kinetic Studies

Figure 1 shows the results of the adsorption kinetic experiments carried out by varying the contact time from 0.5 h to 24 h using 400 mg/L initial concentration. The sorption of CV increased precipitously during the first 30 min of the adsorption process and later slowed until equilibrium was reached. The adsorption rate controlled by intra-particle diffusion involves pore and surface diffusion, which occur coherently within the adsorbent particles [58]. The rapid removal may be attributed to the diffusion of CV to mesopores on the surface of BC-PKS. In our previous study [59], the average pore diameter of BC-PKS was 4.1 nm, which corresponds to mesopores (2–50 nm) as per the classification of the International Union of Pure and Applied Chemistry. The dispersion of CV molecules through the mesopores toward the BC-PKS intra particle matrix caused the removal rate to disinclose because of low dye concentration and fewer adsorption sites [59–61].

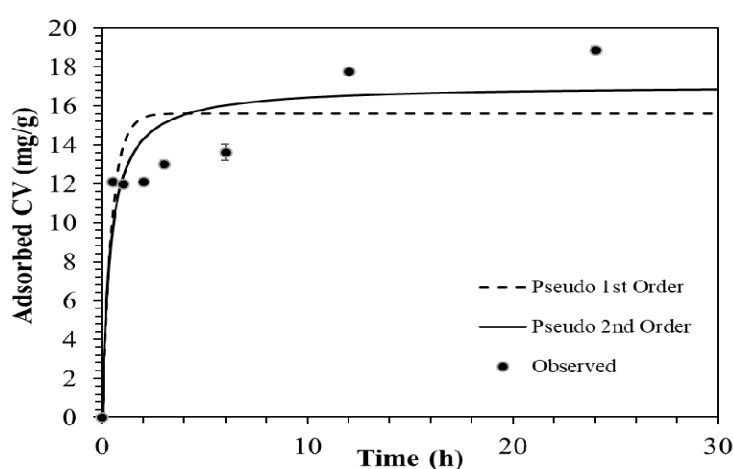


**Figure 1.** The kinetic adsorption of crystal violet (CV) onto biochar derived from palm kernel shell (BC-PKS) with the model fits of the pseudo-first and second-order models (initial concentration: 400 mg/L; volume: 30 mL; adsorbent dosage: 0.5 g; reaction time: 0.5–24 h; temperature: °C).

The pseudo-first- and second-order models were employed to explore the mechanism involved in the adsorption process, and the results are summarized in Table 1. Comparatively, a higher determination coefficient ( $R^2$ ) value was obtained for the pseudo-second-order than for the pseudo-first-order. This implies that the experimental data is a superior fit with pseudo-second-order model for CV adsorption onto BC-PKS and the adsorption process is principally governed by chemisorption through electron sharing between BC-PKS and CV [62–64]. The adsorption of CV to BC-PKS can be explained by ion exchange between deprotonated carboxyl and hydroxyl groups on the surface of BC-PKS and the quaternary amine groups of cationic CV molecule [64]. Similar results have been reported for the sorption of dye onto rice husk [65] and the adsorption of basic dye onto BC-PKS [66].

**Table 1.** Kinetics parameters for CV adsorption onto BC-PKS.

Adsorbent	Pseudo-First-Order			Pseudo-Second-order		
	$q_e$ (mg/g)	$k_1$ (1/h)	$R^2$	$q_e$ (mg/g)	$k_2$ (mg/g/h)	$R^2$
BC-PKS	14.9	2.61	0.817	16.4	0.19	0.884

### 3.2. Adsorption Isotherm

The equilibrium adsorption isotherm experiment was studied under different initial concentrations (50, 100, 200, 300, 400, and 500) mg/L using 0.5 g of BC-PKS per 30 mL of CV solutions at a temperature of 25 °C. The equilibrium adsorption isotherm determines the interrelation between the CV concentration in solution and adsorbed CV on the solid phase in terms of surface property and adsorption affinity [67].

Langmuir and Freundlich isotherms were employed to analyze the equilibrium data, and each isotherm parameter was calculated, as presented in Figure 2 and Table 2. The selection of the better isotherm model fit for adsorption data was based on the determination coefficient value ( $R^2$ ). Fitting the experimental results to Freundlich and Langmuir adsorption isotherms for BC-PKS yielded  $R^2$  values of 0.924 and 0.954, respectively [68]. The Langmuir isotherm model provided a better fit for CV adsorption than the Freundlich isotherm model. The Langmuir isotherm fit indicates a monolayer coverage of CV onto the outer surface of the BC-PKS through uniform CV molecules adsorption onto the surface active sites [69].

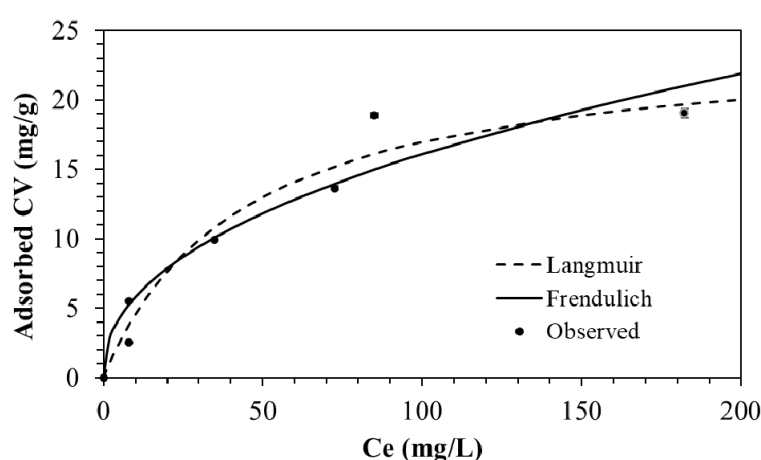


**Figure 2.** CV adsorption to BC-PKS as a function of equilibrium concentration of CV with the Langmuir and Freundlich isotherm model fits (initial concentration: 50–500 mg/L; volume: 30 mL; adsorbent dosage: 0.5 g; reaction time: 24 h; temperature: °C).

**Table 2.** Langmuir and Freundlich constants for CV on BC-PKS.

Adsorbents	Langmuir Isotherm			Freundlich Isotherm		
	$Q_m$ (mg/g)	$K_L$ (L/mg)	$R^2$	$K_F$	$1/n$	$R^2$
BC-PKS	24.45	0.023	0.954	2.07	0.447	0.924

Additionally, the Langmuir isotherm could be used to predict the favorability or unfavorability of the adsorption process when expressed in terms of dimensionless separation parameters  $R_L$  [70].  $R_L$  is defined as follows:

$$R_L = 1/[1 + (K_L \times C_0)], \quad (9)$$

where  $K_L$  is the Langmuir constant, and  $C_0$  is the initial concentration.

Therefore, the calculated  $R_L$  values for initial CV concentrations (50–500 mg/L) ranged from 0.081 to 0.468. Values between 0 and 1 indicate a favorable adsorption of CV onto BC-PKS [71]. A similar phenomenon was reported for the adsorption of direct dye onto rice husk [72] and the adsorption of basic dye onto BC-PKS [66]. Table 2 lists the obtained values of  $1/n$  ( $0.1 < 1/n < 1$ ), indicating strong bonding between BC-PKS and CV.

The maximum CV adsorption capacity was determined to be 24.45 mg/g for BC-PKS, which is comparable to other adsorbents, as shown in Table 3. The low adsorption of BC-PKS may be because of poor surface chemistry resulting from undeveloped porosities and fewer functional groups [73].

Therefore, various modification techniques such as metal oxide impregnation and functionalization can be explored to improve the adsorption capacity [74]. However, millions of tons of PKS is produced annually from oil palm plantations [75]; its use as an adsorbent helps solve the issue of disposal with no environmental impact. Additionally, the particle size and granular nature of BC-PKS allow easy separation in the filtration or precipitation processes when compared to sugar bagasse fiber that can form sludge.

**Table 3.** Comparison of CV adsorption capacity to various adsorbents.

Adsorbent	Adsorption Capacity (mg/g)	Particle Size	pH	Temperature (°C)	Reference
Sugar cane bagasse	692.1	0.075–0.149 mm	7.0	45	[76]
Grapefruit peel	254.16	0.85–1.0 mm	6.0	30 ± 2	[64]
Bamboo leaf	229.35	0.125 mm	7.36	32	[77]
Tea dust	175.4	315–500 µm	7.00	25	[78]
Coffee waste	125	<250 µm	6.00	20 ± 2	[79]
Palm kernel fiber	78.9	50–80 µm	7.20	25 ± 1	[80]
Pineapple leaf powder	78.22	100–125 µm	8.00	20	[81]
Wheat bran	69.15	150–250 µm	10.0	20	[82]
Coir pith	65.53	>600 µm	6.65	30	[8]
Kaolin	47.27	2.37 mm	7.00	22	[83]
NaOH-modified rice husk	44.87	NA	8.00	20	[9]
Jackfruit leaf powder	43.40	100–125 µm	7.00	20	[84]
Rice bran	41.68	150–250 µm	10.0	20	[82]
Himalayan long-leaf pine bark	32.78	0.063–0.355 mm	8.00	30	[1]
BC-PKS	24.45	0.85–1.16 mm	7.00	25	This study
Rubber seed shell	23.81	0.425–2.8 mm	7.00	30 ± 2	[31]
Sugarcane fiber-based	10.44	>600 µm	4.80	30	[8]
Sagaun sawdust	3.50	180 µm	7.50	30 ± 1	[85]
Neem sawdust	4.44–3.99	0.180 mm	7.20	25–45	[86]

### 3.3. Thermodynamics

The influence of thermal temperatures on CV removal by BC-PKS was examined using 30 mL of solution with a 400 mg/L initial concentration, and 0.5 g of BC-PKS at temperatures of 15, 25, and 35 °C. The thermodynamic parameters (Table 4) show negative values for Gibb's free energy change ( $\Delta G^\circ$ ), indicating that CV adsorption onto BC-PKS is feasibly spontaneous. The decrease in the negative values of  $\Delta G^\circ$  with increasing temperature implies a favorable CV adsorption at higher temperatures. This is primarily due to the increased mobility of the CV molecules in solution [87].

**Table 4.** Thermodynamic parameters for adsorption of CV on BC-PKS (initial concentration: 400 mg/L; volume: 30 mL; adsorbent dosage: 0.5 g; reaction time: 24 h; temperature: 15, 25, 35 °C).

Temperature (K)	$\Delta H^\circ$ (kJ/mol)	$\Delta S^\circ$ (kJ/mol·K)	$\Delta G^\circ$ (kJ/mol)
288	60.5	0.214	−1.20
298	-	-	−2.71
308	-	-	−5.50

The values of  $\Delta H^\circ$  and  $\Delta S^\circ$  are estimated from the slope and intercept of the plot of  $\ln K_e$  versus  $1/T$  for CV adsorption onto BC-PKS (Table 4). The positive values of  $\Delta H^\circ$  confirm that the adsorption reactions of CV onto BC-PKS are endothermic, suggesting the adsorption of CV was more favorable with increasing temperature [10,88]. In addition,  $\Delta H^\circ$  was 60.5 kJ/mol, indicating that CV adsorption onto BC-PKS was achieved via chemisorption, which occurs when  $\Delta H^\circ > 40$  kJ/mol [89,90]. The positive values of  $\Delta S^\circ$  for BC-PKS signify an increase in the disorder at the interfaces between CV and BC-PKS during the CV adsorption on BC-PKS that is accompanied with changes in the CV and BC-PKS structures [10,91].



### 3.4. Effects of the pH of the Solution

The adsorption efficiency under different solution pH was investigated because variations in pH affect the degree of ionization of the adsorptive molecule and the BC-PKS surface properties [92]. Thus, adsorption of CV onto BC-PKS at 25 °C with initial dye concentration of 400 mg/L and a BC-PKS dose of 0.5 g was examined by adjusting the solution pH from 2 to 10. The adsorption of CV on BC-PKS increased from 12.4 to 16.4 mg/g when the pH increased from 2 to 4 (Figure 3). Additionally, the percentage removal of CV on BC-PKS increased from 51.8% at pH 2.0 to 68.7% at pH 6.0. CV adsorption on BC-PKS showed a rapid increase in the adsorption capacity and high percentage removal from pH 4 to pH 6, primarily due to the change of surface charge of BC-PKS. The zero point charge of BC-PKS was reported to be 5.50 [93] and 3.94 [94]. As the pH of the CV dye solution increases, the surface of BC-PKS become negatively charged, enhancing the adsorption of the positively charged cationic dye through electrostatic attraction [92,95]. Similar observations were reported in the use of rice husk for the removal of basic dyes from wastewater [96].

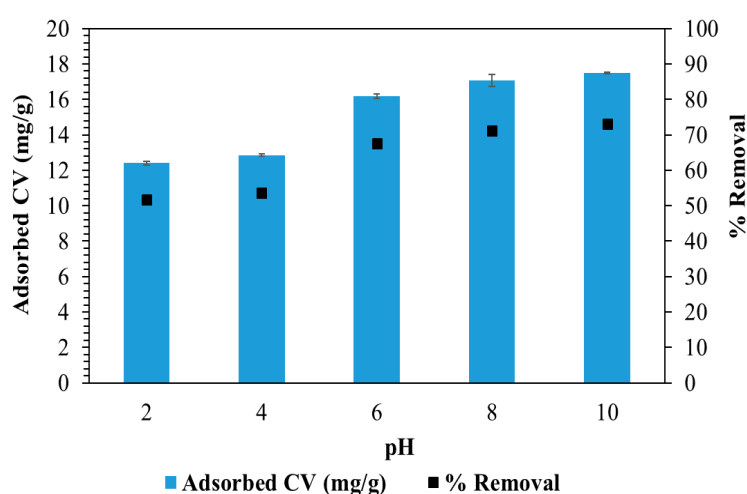


**Figure 3.** Effect of solution pH (2–10) on CV adsorption to BC-PKS (initial concentration: 400 mg/L; volume: 30 mL; adsorbent dosage: 0.5 g; reaction time: 24 h; temperature: 25 °C).

### 3.5. Effect of BC-PKS Dosage

The removal of CV by BC-PKS was studied using six different BC-PKS dosages (0.1–1.0 g) with 30 mL of CV with an initial concentration of 400 mg/L; the results are plotted in Figure 4. The percentage removal of CV increases steadily as the BC-PKS dosage increases because of the increase in the number of adsorption sites [97]. As the BC-PKS dosage increases from 0.1 to 1.0 g, the percentage removal increases from 50.8% to 86.4%. Therefore, 30.9 g/L of BC-PKS dosage is required to remove 80% of the CV. Conversely, an increased BC-PKS dose reduced the amount of CV adsorption to unit mass of BC-PKS from 60.4 mg/g to 10.4 mg/g due to the split in the flux or the concentration gradient between the solute concentration in solution and the solute concentration at the BC-PKS surface [79,98].

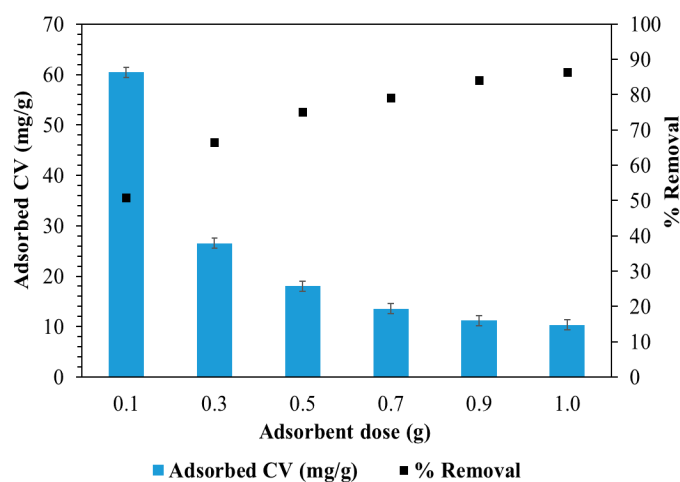


**Figure 4.** Effect of BC-PKS dosage (0.1–1.0 g) on the adsorbed CV per unit mass of BC-PKS (mg/g) and the removal percentage of CV by BC-PKS (%) (initial concentration: 400 mg/L; volume: 30 mL; adsorbent dosage: 0.1–1.0 g; reaction time: 24 h; temperature: 25 °C).

### 3.6. Effect of Competitive Cations

Wastewater from industries contains various contaminants, such as, acids, bases, salts, metal ions, and other inorganic compounds. The existence of cations in the wastewater contributes to a high ionic strength solution [99] that may significantly impact the adsorption capacity of BC-PKS [100]. Therefore, the effect of cations including monovalent ( $\text{Na}^+$ ), divalent ( $\text{Ca}^{2+}$ ), and trivalent ( $\text{Al}^{3+}$ ) ions on the adsorption of CV by BC-PKS were studied. The results as illustrated in Figure 5 demonstrates that BC-PKS adsorption of CV decreased in the presence of  $\text{Na}^+$ ,  $\text{Ca}^{2+}$ , and  $\text{Al}^{3+}$ , indicating the impact of the cations on the adsorption of CV by BC-PKS through a competitive sorption mechanism caused by the reduction in the attraction between active sorption sites and CV molecules [101]. However, the differences in the adsorption amount were more significant with the rise of cationic concentrations because of increased competition for adsorption sites [102]. Additionally, the impact of the co-existing cations on the CV adsorption followed the decreasing order:  $\text{Al}^{3+} > \text{Ca}^{2+} > \text{Na}^+$  because  $\text{Al}^{3+}$  has a higher valence charge than the monovalent ( $\text{Na}^+$ ) and divalent ( $\text{Ca}^{2+}$ ) cations [103].

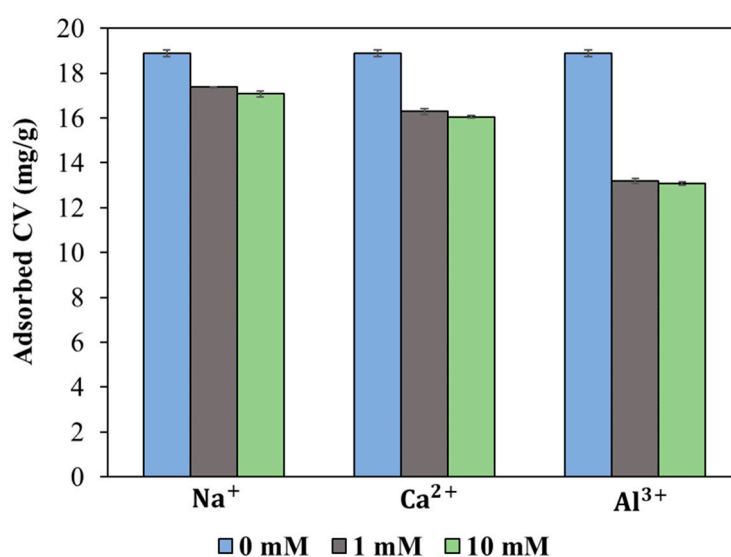


**Figure 5.** Effect of competing cations on CV adsorption on BC-PKS (initial concentration: 400 mg/L; volume: 30 mL; adsorbent dosage: 0.5 g; reaction time: 24 h; temperature: 25 °C).



#### 4. Conclusions

The feasibility of the agricultural by-product PKS for removing CV from textile wastewater was investigated in this study. Kinetic studies revealed that chemisorption is the key limiting factor for the rate of CV adsorption. The equilibrium data were better fitted to the Langmuir model, indicating that CV adsorbed on BC-PKS as a monolayer with uniform CV molecules adsorption. Thermodynamic studies revealed that CV adsorption to BC-PKS was a spontaneous, endothermic process with increasing CV adsorption to BC-PKS at higher temperatures. The increase of solution pH changed the surface charge of BC-PKS, which served favorable adsorption sites for cationic CV dyes via electrostatic attraction. When the BC-PKS loading rate was increased, the percentage of CV removal was found to increase due to the increase of available adsorption sites, but the adsorption capacity began to decrease because of the decline of the flux gradient. The presence of cations in the wastewater decreased the CV adsorption to BC-PKS because of increased competition for adsorption sites. It can be concluded that biochar prepared from the agricultural byproduct has adequate adsorption capacity and can be used as an efficient and cost-effective adsorbent for the removal of CV from textile wastewater.

**Author Contributions:** P.P.K.: Experiment, Data curation; J.O.Q.: Formal analysis, Visualization, Writing-original draft; C.-G.L.: Investigation, Validation; J.-K.M.: Conceptualization, Writing-review & editing; S.-J.P.: Conceptualization, Writing-review & editing, Supervision, Funding acquisition. All authors have read and agreed to the published version of the manuscript.

**Funding:** This research was supported by Basic Science Research Program through the National Research Foundation of Korea (NRF) funded by the Ministry of Education (No. 2017R1D1A1B03030649).

**Conflicts of Interest:** The authors declare no conflict of interest.

#### References

1. Ahmad, R. Studies on adsorption of crystal violet dye from aqueous solution onto coniferous pinus bark powder (CPBP). *J. Hazard. Mater.* **2009**, *171*, 767–773. [\[CrossRef\]](#)
2. Alsenani, G. Studies on adsorption of crystal violet dye from aqueous solution onto calligonum comosum leaf powder (CCLP). *Am. J. Sci.* **2013**, *9*, 30–35.
3. Bhatnagar, A.; Jain, A. A comparative adsorption study with different industrial wastes as adsorbents for the removal of cationic dyes from water. *J. Colloid Interface Sci.* **2005**, *281*, 49–55. [\[CrossRef\]](#)
4. Alizadeh, N.; Shariati, S.; Besharati, N. Adsorption of crystal violet and methylene blue on azolla and fig leaves modified with magnetite iron oxide nanoparticles. *Int. J. Environ. Res.* **2017**, *11*, 197–206. [\[CrossRef\]](#)
5. Nguyen, T.A.; Juang, R.-S. Treatment of waters and wastewaters containing sulfur dyes: A review. *Chem. Eng.* **2013**, *219*, 109–117. [\[CrossRef\]](#)
6. Daneshvar, N.; Oladegaragoze, A.; Djafarzadeh, N. Decolorization of basic dye solutions by electrocoagulation: An investigation of the effect of operational parameters. *J. Hazard. Mater.* **2006**, *129*, 116–122. [\[CrossRef\]](#)
7. Chen, C.-C.; Liao, H.-J.; Cheng, C.-Y.; Yen, C.-Y.; Chung, Y.-C. Biodegradation of crystal violet by *Pseudomonas putida*. *Biotechnol. Lett.* **2007**, *29*, 391–396. [\[CrossRef\]](#)
8. Parab, H.; Sudersanan, M.; Shenoy, N.; Pathare, T.; Vaze, B. Use of agro-industrial wastes for removal of basic dyes from aqueous solutions. *Clean (Weinh)* **2009**, *37*, 963–969. [\[CrossRef\]](#)
9. Chakraborty, S.; Chowdhury, S.; Saha, P.D. Adsorption of crystal violet from aqueous solution onto NaOH-modified rice husk. *Carbohydr. Polym.* **2011**, *86*, 1533–1541. [\[CrossRef\]](#)
10. Mohanty, K.; Naidu, J.T.; Meikap, B.C.; Biswas, M.N. Removal of crystal violet from wastewater by activated carbons prepared from rice husk. *Ind. Eng. Chem. Res.* **2006**, *45*, 5165–5171. [\[CrossRef\]](#)
11. Ali, H.; Muhammad, S.K. Biosorption of crystal violet from water on leaf biomass of *Calotropis procera*. *Environ. Sci. Technol.* **2008**, *1*, 143–150. [\[CrossRef\]](#)
12. Atul, K.; Pratibha, C.; Poonam, V. A comparative study on the treatment methods of textile dye effluents. *Pharm. Res.* **2012**, *4*, 763–771.
13. Lin, S.H.; Chen, M.L. Treatment of textile wastewater by chemical methods for reuse. *Water Res.* **1997**, *31*, 868–876. [\[CrossRef\]](#)

14. Mai, Z. Membrane Processes for Water and Wastewater Treatment: Study and Modeling of Interactions between Membrane and Organic Matter. Ph.D. Thesis, Ecole Centrale Paris, Châtenay-Malabry, France, 2013.
15. Mignani, M.; Nosenzo, G.; Gualdi, A. Innovative ultrafiltration for wastewater reuse. *Desalination* **1999**, *124*, 287–292. [[CrossRef](#)]
16. Stoller, M.; Vilardia, G.; Di, L.; Palmaa, A.C. Treatment of olive oil processing wastewater by ultrafiltration, nanofiltration, reverse osmosis and biofiltration. *Chem. Eng.* **2016**, *47*, 409–414.
17. Pang, Y.L.; Abdullah, A.Z. Current status of textile industry wastewater management and research progress in Malaysia: A review. *Clean (Weinh)* **2013**, *41*, 751–764. [[CrossRef](#)]
18. Homaeigohar, S.; Botcha, N.K.; Zarie, E.; Elbahri, M. Ups and downs of water photodecolorization by nanocomposite polymer nanofibers. *Nanomaterials* **2019**, *9*, 250. [[CrossRef](#)]
19. Das, S. *Textile Effluent Treatment—A Solution to the Environmental Pollution*; Fibre2Fashion: Ahmedabad, India, 2000.
20. Jain, R.; Sharma, N.; Bhargava, M. Electrochemical treatment of effluents from textile and dyeing industries. *J. Sci. Ind. Res.* **2004**, *63*, 405–409.
21. Rafatullah, M.; Sulaiman, O.; Hashim, R.; Ahmad, A. Adsorption of methylene blue on low-cost adsorbents: A review. *J. Hazard. Mater.* **2010**, *177*, 70–80. [[CrossRef](#)]
22. Homaeigohar, S. The nanosized dye adsorbents for water treatment. *Nanomaterials* **2020**, *10*, 295. [[CrossRef](#)]
23. Homaeigohar, S.; Zillohu, A.U.; Abdelaziz, R.; Hedayati, M.K.; Elbahri, M. A novel nanohybrid nanofibrous adsorbent for water purification from dye pollutants. *Materials* **2016**, *9*, 848. [[CrossRef](#)] [[PubMed](#)]
24. Laskar, N.; Kumar, U. Adsorption of crystal violet from wastewater by modified bambusa tulda. *KSCE J. Civ. Eng.* **2018**, *22*, 2755–2763. [[CrossRef](#)]
25. Yagub, M.T.; Sen, T.K.; Afroze, S.; Ang, H.M. Dye and its removal from aqueous solution by adsorption: A review. *Adv. Colloid Interface Sci.* **2014**, *209*, 172–184. [[CrossRef](#)] [[PubMed](#)]
26. Taştan, B.E.; Ertuğrul, S.; Dönmez, G. Effective bioremoval of reactive dye and heavy metals by *Aspergillus versicolor*. *Bioresour. Technol.* **2010**, *101*, 870–876. [[CrossRef](#)]
27. Choy, K.K.; McKay, G.; Porter, J.F. Sorption of acid dyes from effluents using activated carbon. *Resour. Conserv. Recycl.* **1999**, *27*, 57–71. [[CrossRef](#)]
28. Liu, N.; Charrua, A.B.; Weng, C.-H.; Yuan, X.; Ding, F. Characterization of biochars derived from agriculture wastes and their adsorptive removal of atrazine from aqueous solution: A comparative study. *Bioresour. Technol.* **2015**, *198*, 55–62. [[CrossRef](#)]
29. Jung, C.; Park, J.; Lim, K.H.; Park, S.; Heo, J.; Her, N.; Oh, J.; Yun, S.; Yoon, Y. Adsorption of selected endocrine disrupting compounds and pharmaceuticals on activated biochars. *J. Hazard. Mater.* **2013**, *263*, 702–710. [[CrossRef](#)]
30. Zheng, W.; Guo, M.; Chow, T.; Bennett, D.N.; Rajagopalan, N. Sorption properties of greenwaste biochar for two triazine pesticides. *J. Hazard. Mater.* **2013**, *263*, 702–710. [[CrossRef](#)]
31. Tan, I.; Hameed, B. Removal of crystal violet dye from aqueous solutions using rubber (*Hevea brasillensis*) seed shell-based biosorbent. *Desalin. Water Treat.* **2012**, *48*, 174–181. [[CrossRef](#)]
32. Ullah, I.; Nadeem, R.; Iqbal, M.; Manzoor, Q. Biosorption of chromium onto native and immobilized sugarcane bagasse waste biomass. *Ecol. Eng.* **2013**, *60*, 99–107. [[CrossRef](#)]
33. Manzoor, Q.; Nadeem, R.; Iqbal, M.; Saeed, R.; Ansari, T.M. Organic acids pretreatment effect on *Rosa bourbonia* phyto-biomass for removal of Pb(II) and Cu(II) from aqueous media. *Bioresour. Technol.* **2013**, *132*, 446–452. [[CrossRef](#)] [[PubMed](#)]
34. Song, J.; Zou, W.; Bian, Y.; Su, F.; Han, R. Adsorption characteristics of methylene blue by peanut husk in batch and column modes. *Desalination* **2011**, *265*, 119–125. [[CrossRef](#)]
35. Fan, X.; Parker, D.J.; Smith, M.D. Adsorption kinetics of fluoride on low cost materials. *Water Res.* **2003**, *37*, 4929–4937. [[CrossRef](#)] [[PubMed](#)]
36. Wang, Z.; Han, P.; Jiao, Y.; Ma, D.; Dou, C.; Han, R. Adsorption of congo red using ethylenediamine modified wheat straw. *Desalin. Water Treat.* **2011**, *30*, 195–206. [[CrossRef](#)]
37. Ramakrishnan, M.; Nagarajan, S. Utilization of waste biomass for the removal of basic dye from water. *World Appl. Sci. J.* **2009**, *5*, 114–120.
38. Sewu, D.D.; Boakye, P.; Woo, S.H. Highly efficient adsorption of cationic dye by biochar produced with Korean cabbage waste. *Bioresour. Technol.* **2017**, *224*, 206–213. [[CrossRef](#)]

39. Vyavahare, G.; Jadhav, P.; Jadhav, J.; Patil, R.; Aware, C.; Patil, D.; Gophane, A.; Yang, Y.-H.; Gurav, R. Strategies for crystal violet dye sorption on biochar derived from mango leaves and evaluation of residual dye toxicity. *J. Clean. Prod.* **2019**, *207*, 296–305. [[CrossRef](#)]
40. Wathukarage, A.; Herath, I.; Iqbal, M.C.M.; Vithanage, M. Mechanistic understanding of crystal violet dye sorption by woody biochar: Implications for wastewater treatment. *Environ. Geochem. Health* **2019**, *41*, 1647–1661. [[CrossRef](#)]
41. Bernardino, C.A.R.; Mahler, C.F.; Veloso, M.C.C.; Romeiro, G.A. Preparation of biochar from sugarcane by-product filter mud by slow pyrolysis and its use like adsorbent. *Waste Biomass Valoriz.* **2017**, *8*, 2511–2521. [[CrossRef](#)]
42. Sewu, D.D.; Jung, H.; Kim, S.S.; Lee, D.S.; Woo, S.H. Decolorization of cationic and anionic dye-laden wastewater by steam-activated biochar produced at an industrial-scale from spent mushroom substrate. *Bioresour. Technol.* **2019**, *277*, 77–86. [[CrossRef](#)]
43. Leng, L.; Yuan, X.; Zeng, G.; Shao, J.; Chen, X.; Wu, Z.; Wang, H.; Peng, X. Surface characterization of rice husk bio-char produced by liquefaction and application for cationic dye (*Malachite green*) adsorption. *Fuel* **2015**, *155*, 77–85. [[CrossRef](#)]
44. Vu, T.M.; Doan, D.P.; Van, H.T.; Nguyen, T.V.; Vigneswaran, S.; Ngo, H.H. Removing ammonium from water using modified corncob-biochar. *Sci. Total Environ.* **2017**, *579*, 612–619. [[CrossRef](#)] [[PubMed](#)]
45. Ahmad, M.; Lee, S.S.; Oh, S.-E.; Mohan, D.; Moon, D.H.; Lee, Y.H.; Ok, Y.S. Modeling adsorption kinetics of trichloroethylene onto biochars derived from soybean stover and peanut shell wastes. *Environ. Sci. Pollut. Res.* **2013**, *20*, 8364–8373. [[CrossRef](#)] [[PubMed](#)]
46. Mahdi, Z.; Yu, Q.J.; El Hanandeh, A. Investigation of the kinetics and mechanisms of nickel and copper ions adsorption from aqueous solutions by date seed derived biochar. *J. Environ. Chem. Eng.* **2018**, *6*, 1171–1181. [[CrossRef](#)]
47. Yang, H.I.; Lou, K.; Rajapaksha, A.U.; Ok, Y.S.; Anyia, A.O.; Chang, S.X. Adsorption of ammonium in aqueous solutions by pine sawdust and wheat straw biochars. *Environ. Sci. Pollut. Res.* **2018**, *25*, 25638–25647. [[CrossRef](#)]
48. Vidhya, L.; Dhandapani, M. Removal of Cr (VI) from aqueous solution using coir pith biochar—An eco-friendly approach. *Indian J. Chem. Technol.* **2018**, *25*, 266–273.
49. Ahmadi, M.; Kouhgard, E.; Ramavandi, B. Physico-chemical study of dew melon peel biochar for chromium attenuation from simulated and actual wastewaters. *Korean J. Chem. Eng.* **2016**, *33*, 2589–2601. [[CrossRef](#)]
50. Rashidi, N.A.; Yusup, S. Potential of palm kernel shell as activated carbon precursors through single stage activation technique for carbon dioxide adsorption. *J. Clean. Prod.* **2017**, *168*, 474–486. [[CrossRef](#)]
51. Bakar, A.H.B.A.; Koay, Y.S.; Ching, Y.C.; Abdullah, L.C.; Choong, T.S.; Alkhatib, M.A.; Mobarekeh, M.N.; Zahri, N.A.M. Removal of fluoride using quaternized palm kernel shell as adsorbents: Equilibrium isotherms and kinetics studies. *Bioresources* **2016**, *11*, 4485–4511.
52. Hamza, U.D.; Nasri, N.S.; Amin, N.S.; Mohammed, J.; Zain, H.M. Characteristics of oil palm shell biochar and activated carbon prepared at different carbonization times. *Desalin. Water Treat.* **2016**, *57*, 7999–8006. [[CrossRef](#)]
53. Uttran, A.; Loh, S.; Kong, S.; Bachmann, R. Adsorption of npk fertiliser and humic acid on palm kernel shell biochar. *J. Oil Palm Res.* **2018**, *30*, 472–484.
54. APHA. *Standard Methods for the Examination of Water and Wastewater*; American Public Health Association: Washington, DC, USA, 1995.
55. Triwiswara, M.; Lee, C.-G.; Moon, J.-K.; Park, S.-J. Adsorption of triclosan from aqueous solution onto char derived from palm kernel shell. *Desalin. Water Treat.* **2020**, *177*, 71–79. [[CrossRef](#)]
56. Lee, J.-I.; Hong, S.-H.; Lee, C.-G.; Park, S.-J. Experimental and model study for fluoride removal by thermally activated sepiolite. *Chemosphere* **2020**, *241*, 125094. [[CrossRef](#)] [[PubMed](#)]
57. Vilardi, G.; Di Palma, L.; Verdone, N. Heavy metals adsorption by banana peels micro-powder: Equilibrium modeling by non-linear models. *Chin. J. Chem. Eng.* **2018**, *26*, 455–464. [[CrossRef](#)]
58. Ali, R.M.; Hamad, H.A.; Hussein, M.M.; Malash, G.F. Potential of using green adsorbent of heavy metal removal from aqueous solutions: Adsorption kinetics, isotherm, thermodynamic, mechanism and economic analysis. *Ecol. Eng.* **2016**, *91*, 317–332. [[CrossRef](#)]
59. Gong, R.; Zhu, S.; Zhang, D.; Chen, J.; Ni, S.; Guan, R. Adsorption behavior of cationic dyes on citric acid esterifying wheat straw: Kinetic and thermodynamic profile. *Desalination* **2008**, *230*, 220–228. [[CrossRef](#)]

60. Toor, M.; Jin, B. Adsorption characteristics, isotherm, kinetics, and diffusion of modified natural bentonite for removing diazo dye. *Chem. Eng.* **2012**, *187*, 79–88. [[CrossRef](#)]
61. Liu, W.; Hu, R.; Li, Y.; Huang, Y.; Wang, Y.; Wei, Z.; Yu, E.; Guo, X. Cross-linking of poly (dimethylaminoethyl methacrylate) by phytic acid: pH-responsive adsorbent for high-efficiency removal of cationic and anionic dyes. *RSC Adv.* **2020**, *10*, 4232–4242. [[CrossRef](#)]
62. Ho, Y.-S.; McKay, G. Pseudo-second order model for sorption processes. *Process Biochem.* **1999**, *34*, 451–465. [[CrossRef](#)]
63. Aysan, H.; Edeballi, S.; Ozdemir, C.; Celik Karakaya, M.; Karakaya, N. Use of chabazite, a naturally abundant zeolite, for the investigation of the adsorption kinetics and mechanism of methylene blue dye. *Microporous Mesoporous Mater.* **2016**, *235*, 78–86. [[CrossRef](#)]
64. Saeed, A.; Sharif, M.; Iqbal, M. Application potential of grapefruit peel as dye sorbent: Kinetics, equilibrium and mechanism of crystal violet adsorption. *J. Hazard. Mater.* **2010**, *179*, 564–572. [[CrossRef](#)] [[PubMed](#)]
65. Sawasdee, S.; Jankerd, H.; Watcharabundit, P. Adsorption of dyestuff in household-scale dyeing onto rice husk. *Energy Proced.* **2017**, *138*, 1159–1164. [[CrossRef](#)]
66. Jumasiah, A.; Chuah, T.; Gimbon, J.; Choong, T.; Azni, I. Adsorption of basic dye onto palm kernel shell activated carbon: Sorption equilibrium and kinetics studies. *Desalination* **2005**, *186*, 57–64. [[CrossRef](#)]
67. Han, X.; Niu, X.; Ma, X. Adsorption characteristics of methylene blue on poplar leaf in batch mode: Equilibrium, kinetics and thermodynamics. *Korean J. Chem. Eng.* **2012**, *29*, 494–502. [[CrossRef](#)]
68. Chen, S.; Yue, Q.; Gao, B.; Li, Q.; Xu, X. Removal of Cr(VI) from aqueous solution using modified corn stalks: Characteristic, equilibrium, kinetic and thermodynamic study. *Chem. Eng.* **2011**, *168*, 909–917. [[CrossRef](#)]
69. Duraisamy, R.; Kiruthiga, P.; Hirpaye, B.; Berekute, A. Adsorption of azure B dye on rice husk activated carbon: Equilibrium, kinetic and thermodynamic studies. *Int. J. Water Res.* **2015**, *5*, 8–28.
70. Shoukat, S.; Bhatti, H.N.; Iqbal, M.; Noreen, S. Mango stone biocomposite preparation and application for crystal violet adsorption: A mechanistic study. *Microporous Mesoporous Mater.* **2017**, *239*, 180–189. [[CrossRef](#)]
71. Lee, C.-G.; Hong, S.-H.; Hong, S.-G.; Choi, J.-W.; Park, S.-J. Production of biochar from food waste and its application for phenol removal from aqueous solution. *Water Air Soil Pollut.* **2019**, *230*, 70. [[CrossRef](#)]
72. Abdelwahab, O.; El Nemr, A.; El Sikaily, A.; Khaled, A. Use of rice husk for adsorption of direct dyes from aqueous solution: A case study of Direct F. Scarlet. *Egypt. J. Aquat. Res.* **2005**, *31*, 1–11.
73. Wang, L.; Yan, W.; He, C.; Wen, H.; Cai, Z.; Wang, Z.; Chen, Z.; Liu, W. Microwave-assisted preparation of nitrogen-doped biochars by ammonium acetate activation for adsorption of acid red 18. *Appl. Surf. Sci.* **2018**, *433*, 222–231. [[CrossRef](#)]
74. Xue, L.; Gao, B.; Wan, Y.; Fang, J.; Wang, S.; Li, Y.; Muñoz-Carpena, R.; Yang, L. High efficiency and selectivity of MgFe-LDH modified wheat-straw biochar in the removal of nitrate from aqueous solutions. *J. Taiwan Inst. Chem. Eng.* **2016**, *63*, 312–317. [[CrossRef](#)]
75. Mohammad Razi, M.A.; Al-Gheethi, A.; Al-Qaini, M.; Yousef, A. Efficiency of activated carbon from palm kernel shell for treatment of greywater. *Arab. J. Basic Appl. Sci.* **2018**, *25*, 103–110. [[CrossRef](#)]
76. Ferreira, B.C.S.; Teodoro, F.S.; Mageste, A.B.; Gil, L.F.; de Freitas, R.P.; Gurgel, L.V.A. Application of a new carboxylate-functionalized sugarcane bagasse for adsorptive removal of crystal violet from aqueous solution: Kinetic, equilibrium and thermodynamic studies. *Ind. Crops Prod.* **2015**, *65*, 521–534. [[CrossRef](#)]
77. Ghosh, S.K.; Hajra, A.K.; Bandyopadhyay, A. Air agitated tapered bubble column adsorber for hazardous dye (Crystal violet) removal onto activated (ZnCl<sub>2</sub>) carbon prepared from bamboo leaves. *J. Mol. Liq.* **2017**, *240*, 313–321. [[CrossRef](#)]
78. Khan, M.M.R.; Rahman, M.W.; Ong, H.R.; Ismail, A.B.; Cheng, C.K. Tea dust as a potential low-cost adsorbent for the removal of crystal violet from aqueous solution. *Desalin. Water Treat.* **2016**, *57*, 14728–14738. [[CrossRef](#)]
79. Lafi, R.; ben Fradj, A.; Hafiane, A.; Hameed, B. Coffee waste as potential adsorbent for the removal of basic dyes from aqueous solution. *Korean J. Chem. Eng.* **2014**, *31*, 2198–2206. [[CrossRef](#)]
80. El-Sayed, G.O. Removal of methylene blue and crystal violet from aqueous solutions by palm kernel fiber. *Desalination* **2011**, *272*, 225–232. [[CrossRef](#)]
81. Chakraborty, S.; Chowdhury, S.; Saha, P.D. Insight into biosorption equilibrium, kinetics and thermodynamics of crystal violet onto *Ananas comosus* (pineapple) leaf powder. *Appl. Water Sci.* **2012**, *2*, 135–141. [[CrossRef](#)]
82. Wang, X.S.; Liu, X.; Wen, L.; Zhou, Y.; Jiang, Y.; Li, Z. Comparison of basic dye crystal violet removal from aqueous solution by low-cost biosorbents. *Sep. Sci. Technol.* **2008**, *43*, 3712–3731. [[CrossRef](#)]



83. Nandi, B.; Goswami, A.; Das, A.; Mondal, B. Purkait, M. Kinetic and equilibrium studies on the adsorption of crystal violet dye using kaolin as an adsorbent. *Sep. Sci. Technol.* **2008**, *43*, 1382–1403. [\[CrossRef\]](#)
84. Saha, P.D.; Chakraborty, S.; Chowdhury, S. Batch and continuous (fixed-bed column) biosorption of crystal violet by *Artocarpus heterophyllus* (jackfruit) leaf powder. *Colloids Surf. B Biointerfaces* **2012**, *92*, 262–270. [\[CrossRef\]](#) [\[PubMed\]](#)
85. Khattri, S.; Singh, M. Use of Sagaun sawdust as an adsorbent for the removal of crystal violet dye from simulated wastewater. *Environ. Prog. Sustain. Energy* **2012**, *31*, 435–442. [\[CrossRef\]](#)
86. Khattri, S.D.; Singh, M.K. Colour removal from synthetic dye wastewater using a bioadsorbent. *Water Air Soil Pollut.* **2000**, *120*, 283–294. [\[CrossRef\]](#)
87. Aysu, T.; Küçük, M. Removal of crystal violet and methylene blue from aqueous solutions by activated carbon prepared from *Ferula orientalis*. *Int. J. Environ. Sci. Technol.* **2015**, *12*, 2273–2284. [\[CrossRef\]](#)
88. Gerçel, Ö.; Gerçel, H.F.; Koparal, A.S.; Ögütveren, Ü.B. Removal of disperse dye from aqueous solution by novel adsorbent prepared from biomass plant material. *J. Hazard. Mater.* **2008**, *160*, 668–674. [\[CrossRef\]](#)
89. Navarathna, C.M.; Karunanayake, A.G.; Gunatilake, S.R.; Pittman, C.U., Jr.; Perez, F.; Mohan, D.; Mlsna, T. Removal of Arsenic (III) from water using magnetite precipitated onto Douglas fir biochar. *J. Environ. Manag.* **2019**, *250*, 109429. [\[CrossRef\]](#)
90. Monárrez-Cordero, B.E.; Sáenz-Trevizo, A.; Bautista-Carrillo, L.M.; Silva-Vidaurre, L.G.; Miki-Yoshida, M.; Amézaga-Madrid, P. Simultaneous and fast removal of  $As^{3+}$ ,  $As^{5+}$ ,  $Cd^{2+}$ ,  $Cu^{2+}$ ,  $Pb^{2+}$  and  $F^{-}$  from water with composite Fe-Ti oxides nanoparticles. *J. Alloys Compd.* **2018**, *757*, 50–160. [\[CrossRef\]](#)
91. Hong, S.; Wen, C.; He, J.; Gan, F.; Ho, Y.-S. Adsorption thermodynamics of methylene blue onto bentonite. *J. Hazard. Mater.* **2009**, *167*, 630–633. [\[CrossRef\]](#)
92. Nandi, B.; Goswami, A.; Purkait, M. Removal of cationic dyes from aqueous solutions by kaolin: Kinetic and equilibrium studies. *Appl. Clay Sci.* **2009**, *42*, 583–590. [\[CrossRef\]](#)
93. Adebayo, O.; Adaramodu, A.; Ajayi, M.; Olasehinde, F.; Oyetunde, J. Purification of nitrate-contaminated aqueous solution using modified and unmodified palm kernel shell. *Int. Lett. Chem. Phys. Astron.* **2016**, *71*, 11–18. [\[CrossRef\]](#)
94. Anyika, C.; Asri, N.A.M.; Majid, Z.A.; Jaafar, J.; Yahya, A. Batch sorption-desorption of As (III) from waste water by magnetic palm kernel shell activated carbon using optimized Box–Behnken design. *Appl. Water Sci.* **2017**, *7*, 4573–4591. [\[CrossRef\]](#)
95. Salleh, M.A.M.; Mahmoud, D.K.; Karim, W.A.W.A.; Idris, A. Cationic and anionic dye adsorption by agricultural solid wastes: A comprehensive review. *Desalination* **2011**, *280*, 1–13. [\[CrossRef\]](#)
96. Singh, D.; Srivastava, B. Basic dyes removal from wastewater by adsorption on rice husk carbon. *Indian J. Chem. Technol.* **2001**, *8*, 133–139.
97. Yagub, M.T.; Sen, T.K.; Ang, H. Equilibrium, kinetics, and thermodynamics of methylene blue adsorption by pine tree leaves. *Water Air Soil Pollut.* **2012**, *223*, 5267–5282. [\[CrossRef\]](#)
98. Vadivelan, V.; Kumar, K.V. Equilibrium, kinetics, mechanism, and process design for the sorption of methylene blue onto rice husk. *J. Colloid Interface Sci.* **2005**, *286*, 90–100. [\[CrossRef\]](#) [\[PubMed\]](#)
99. Maurya, N.S.; Mittal, A.K.; Cornel, P.; Rother, E. Biosorption of dyes using dead macro fungi: Effect of dye structure, ionic strength and pH. *Bioresour. Technol.* **2006**, *97*, 512–521. [\[CrossRef\]](#) [\[PubMed\]](#)
100. Radovic, L.R.; Moreno-Castilla, C.; Rivera-Utrilla, J. Carbon materials as adsorbents in aqueous solutions. *Chem. Phys. Carbon.* **2001**, *27*, 227–406.
101. Gong, R.; Ding, Y.; Li, M.; Yang, C.; Liu, H.; Sun, Y. Utilization of powdered peanut hull as biosorbent for removal of anionic dyes from aqueous solution. *Dyes Pigments* **2005**, *64*, 187–192. [\[CrossRef\]](#)
102. Antelo, J.; Avena, M.; Fiol, S.; López, R.; Arce, F. Effects of pH and ionic strength on the adsorption of phosphate and arsenate at the goethite–water interface. *J. Colloid Interface Sci.* **2005**, *285*, 476–486. [\[CrossRef\]](#)
103. El-Aassar, M.; El-Kady, M.; Hassan, H.S.; Al-Deyab, S.S. Synthesis and characterization of surface modified electrospun poly (acrylonitrile-co-styrene) nanofibers for dye decolorization. *J. Taiwan Inst. Chem. Eng.* **2016**, *58*, 274–282. [\[CrossRef\]](#)

